Proceedings of the 7th International Conference on Geotechnical and Geophysical Site Characterization
Barcelona, 18 - 21 June 2024

A CT-based approach to evaluate sample quality in soft soils

Jubert Pineda[1#], *Nuria* Sau[2], *Kaiwen* Ouyang[1], and *Marcos* Arroyo[2]

[1]*Priority Research Centre for Geotechnical Science and Engineering, The University of Newcastle Australia, Callaghan Campus, 2308, NSW, Australia*
[2]*Universitat Politécnica de Catalunya, UPC, BarcelonaTech, Barcelona, Spain*

[#]*Corresponding author: Jubert.pineda@newcastle.edu.au*

ABSTRACT

The paper discusses the performance of a novel tool based on computed tomography (CT) to evaluate sample quality in soft soils. This new technique is applied to the low-plasticity Mediterranean deltaic deposits found in the region of Castello d'Empuries at the Costa Brava, in Catalonia (Spain). Tube specimens of variable diameters retrieved using open samplers (Shelby) as well as Osterberg-type fixed-piston samplers were scanned in this study. Statistical analysis of the CT images allows to define a quantitative index of sample quality. Sample quality classification based on this new non-destructive CT-based measure compares well with quality classification based on the well-established recompression sample quality index, $\Delta e/e_0$.

Keywords: sample disturbance, CT scanning, tube sampling, silty deposits, soft soils.

1. Introduction

Despite the vast amount of work carried out in past decades to understand the phenomenon of sampling disturbance in soft soils (e.g. Hvorslev, 1948; Baligh et al., 1987; Lunne et al., 1997; Clayton et al., 1998; Ladd and DeGroot, 2003; Pineda et al., 2016a; Lim et al., 2018, 2019; Monforte et al. 2022), many aspects of this problem are still difficult to address in geotechnical practice. For instance, it would be desirable to have a rapid and reliable method to identify specimen quality before testing. However, the most accepted criterion to evaluate sample disturbance for fine-grained soils remains the sample quality index proposed by Lunne et al. (1997). This index is based on the change in void ratio required to recompress the soil to its in situ stress state. Therefore the evaluation of each tested specimen quality is only obtained after the mechanical test is complete, which is far from ideal.

This paper describes a simple non-destructive methodology to evaluate test specimen quality before testing, based on CT scanning. The methodology is applied in this paper to complex silty deposit from the Costa Brava in Spain where tube samples were obtained using open samplers and fixed piston samplers.

2. Quantitative assessment of sample quality via CT scanning

Ouyang et al. (2024) proposed a simple yet versatile approach to evaluate the disturbance caused by tube sampling in soft soils via CT scanning. This non-destructive technique is based on Beer's law, which relates the incident intensity (I_0) and transmitted intensity (I) of a X or gamma-ray beam passing through an entire transverse section by means of a linear attenuation coefficient (γ) (e.g. Duliu, 1999):

$$I = I_0 \exp\left(-\gamma . x\right) \quad (1)$$

where x is the sample width. The tomographic algorithm attributes a representative attenuation value coefficient μ to every voxel in the image, typically expressed in Hounsfield units. These values are then usually interpreted in terms of soil bulk density, for which purpose a relatively involved calibration is necessary (e.g. Sau, 2013), as the relation between attenuation and bulk density is strongly soil dependent.

The proposed approach for sample evaluation does not require the evaluation of soil density and instead it carries out an statistical analysis of the scanned image in terms of attenuation intensity. Statistical descriptors of attenuation are thus estimated for each slice (2D image) of the 3D stack to obtain: (i) mean CT value μ, (ii) standard deviation σ, and (iii) coefficient of variation *CoV*. Those descriptions are calculated as:

$$\mu = \frac{\sum_{i=1}^{n} CT_i}{n} \quad (2)$$

$$\sigma = \sqrt{\frac{\sum_{i=1}^{n}(CT_i-\mu)^2}{n}} \quad (3)$$

$$CoV = \frac{\sigma}{\mu} \quad (4)$$

where CT_i is the CT value for voxel i in the corresponding CT slice, n is the number of voxels.

Ouyang et al. (2024) proposed the use of *CoV* as a predictor of sample quality as it considers not only the mean CT value but also its variation within a given cross-section area (slice). Results obtained for Ballina clay, a natural (structured) high plasticity soft clay from New South Wales in Australia, showed that values of *CoV* < 0.1 seem to represent well specimens of good quality that could be used for mechanical testing in the laboratory. The estimation of μ, σ and *CoV* is based on pixels only within a Region of Interest (RoI), which is assumed axisymmetric and defined by selecting a fraction of the tube radius. As discussed in Ouyang et al. (2024) the RoI should approximately correspond to the diameter of the soil specimens used in laboratory tests (oedometer or triaxial tests). RoIs should also be defined so as to exclude the area of the sample that is close to the tube wall, as this is highly affected by the strong contrast in density between the tube (typically made of steel) and the soil, introducing a noisy artefact known as "cupping artifact" (Sau, 2013).

This methodology has been recently implemented in a Matlab® code that generates profiles of μ, σ and *CoV* for visualization and quantitative analysis. Figure 1 shows profiles obtained for a tube specimen of Ballina clay which represents the natural soft soil deposits encountered along the east coastline in Australia. Tube specimens of Ballina clay were retrieved using an 89mm fixed-piston sampler (see Pineda et al., 2016b). In Figure 1, a region of interest RoI=0.62 (inner diameter of 55 mm with respect to the 89 mm sample diameter), was adopted. The mean CT value ranges around 1100 HU (Hounsfield units) and remains relatively constant along the tube. The standard deviation σ varies around 50 HU whereas the *CoV* is lower than 0.1 except at both tube ends where soil disturbance is typically high. The fact that *CoV* < 0.1 for most of the tube suggest low sample disturbance, which gives confidence for the selection of specimens for laboratory testing, as it should be expected for fixed-piston samples.

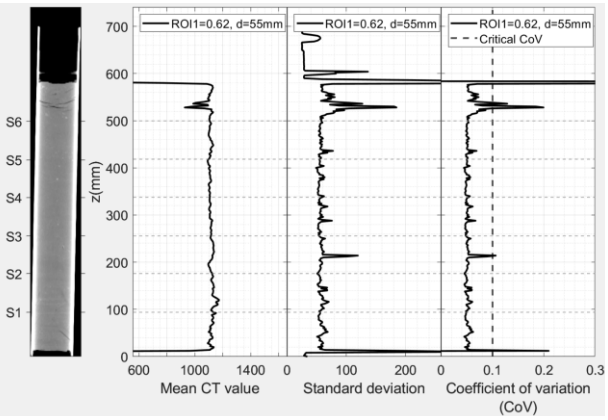

Figure 1. CT scan profiles for a Ballina clay specimen retrieved using a 89mm fixed-piston sampler.

3. Application to natural silty deposits from Spain

The method described above has been applied in this paper to evaluate the quality of tube specimens retrieved from a test site located in the vicinity of Castello d'Empuries in the flat central section of the Costa Brava, Catalonia (Spain). The test site comprises an alluvial plain that forms a typical Mediterranean deltaic environment (see Figure 2) (Diaz & Ercilla, 1993). The soil profile at the test site is composed by silt-clay soils (coastal marsh) interbedded with sand-dominated deposits. Typical thickness for the soft soil stratum ranges around 20-30 m.

Figure 3 shows the variation in clay and silt contents at the test site, obtained from grain size distribution analysis (see Arroyo et al., 2015). Fine grained levels dominate at 2-6 m and again at 12-14 m depth. These levels are classified as low plasticity clays (CL). Index and compositional properties are summarized in Table 1.

Table 1. Index properties of tested horizons

Depth (m)	w_L (%)	PI (%)	Silt (%)	Clay (%)	Carbonates (%)
5-6	34	15	50	18	25
13-14	38	21	66	24	17

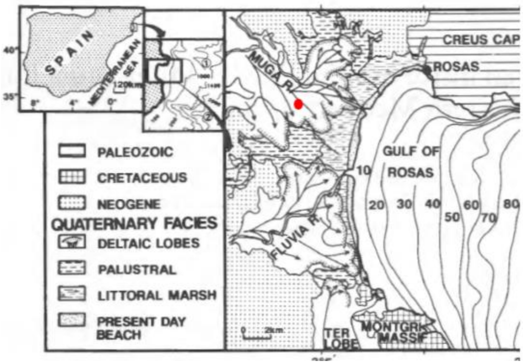

Figure 2. Geological environment and location of the test facility (modified from Diaz and Ercilla, 1993).

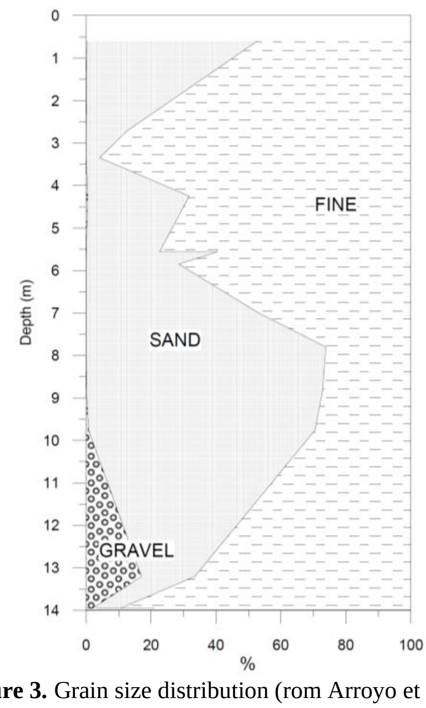

Figure 3. Grain size distribution (rom Arroyo et al., 2015)

3.1. Tube sampling campaign

Tube specimens were retrieved from target depths using two tube sampling methods: (i) two open samplers (Shelby tubes) (80 mm and 89 mm in external diameter), and (ii) two fixed-piston samplers (80 mm and 100 mm in external diameter), of the type described by Osterberg (1973). Samplers were lowered into a pre-drilled hole just above the sampling horizon. Table 2 summarizes the geometry of each sampler including the external diameter (D_e), internal diameter (D_i), thickness of the tube wall (t), tube length (L), area ratio (AR), taper angle β, and inside clearance (ICR). The comparison of those geometric descriptors against values recommended by Ladd and DeGroot (2003) (D_e/t>40, AR≈10%, ICR=0 and β<10°), suggest that relatively small sample disturbance should be expected. After sampling, tubes specimens were stored and extruded vertically. Results for representative tube samples retrieved from 4 boreholes at depths between 5.4–6.1m and 13.5 – 14.1m are presented below.

Table 2. Characteristics of employed tube samplers

Type	D_e (mm)	D_i (mm)	t (mm)	L (mm)	AR (%)	ICR (%)	β (°)
S	88.6	83.5	2.5	600	13	0	~5
S	80.3	76	2.2		12	0	~5
O	80	76	2		11	0	~5
O	100	95	2.5		12	0	~5

S: Shelby sampler ; O: fixed-piston sampler

3.2. Scanning of tube samples

Before mechanical testing, each tube was scanned using a medical CT scanner (Siemens Somaton Spirit®). Scans were performed using 130 keV maximum energy, 63 mA tube current and radiographic exposure of 31 mA.s., reconstruction matrix of 512x512, with in-plane resolution of 0.32x0.32 mm^2, slice width of 3 mm with an increment of 1.5 mm (i.e. two consecutive slices overlap by 50%). Further details are given in Sau (2013).

3.3. Laboratory testing campaign

Constant Rate of Strain (CRS) oedometer tests and K_0-consolidated undrained (CK_0U) triaxial tests were carried out to study the consequences of tub sampling in the silty deposits from Castello d'Empuries. Apart from one tube (Shelby 88 mm retrieved from BH1 at z= 5.5m; see Table 3), CRS and triaxial specimens were obtained from small cylindrical segments (40 mm or 120 mm) sliced using a hand grinder (to cut the tube wall) and a wire saw (to cut the soil). The tube mentioned above was cut alongside its longitudinal axis using a hand grinder. Implications of extrusion method are discussed below.

Oedometer specimens (50 mm in diameter and 20 mm in height) were trimmed by gently pushing a 1 mm-thick oedometer ring into a 40 mm slice (see Figure 4a). The thin oedometer ring (area ratio around 9%) was designed to reduce soil disturbance during sample preparation (Pineda et al., 2012a).

Triaxial samples were trimmed from 120 mm long segments sliced as described above. The soil within each slice was extruded by pushing a steel piston at constant displacement rate (2 mm/min) using a load frame as indicated in Figure 4b. Triaxial specimens (38 mm in diameter and 76 mm in height) were then recompressed under K_0-consolidation to their estimated in situ stress state before undrained shearing.

Detailed analysis of the CRS and CK_0U tests results is presented in Pineda et al. (2012b). This paper only reports the estimated sample quality index ($\Delta e/e_0$) for CRS and CK_0U tests which are compared here against interpreted CT data. The sample quality index ($\Delta e/e_0$) (Lunne et al., 1997) uses void ratio change after recompression to in situ effective stress normalized by the initial void ratio. For soils with overconsolidation ratio OCR<2, four levels of sample quality are specified as follows: *very good to excellent* ($\Delta e/e_0$ < 0.04), *good to fair* (0.04 < $\Delta e/e_0$ < 0.07), *poor* (0.07 < $\Delta e/e_0$ < 0.14) and *very poor* ($\Delta e/e_0$ > 0.14).

Table 3 summarizes the initial conditions of CRS and CK_0U specimens and the estimated $\Delta e/e_0$ for the Shelby and fixed-piston samples reported in this paper.

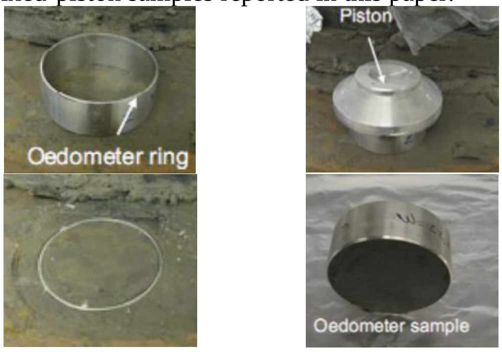

(a)

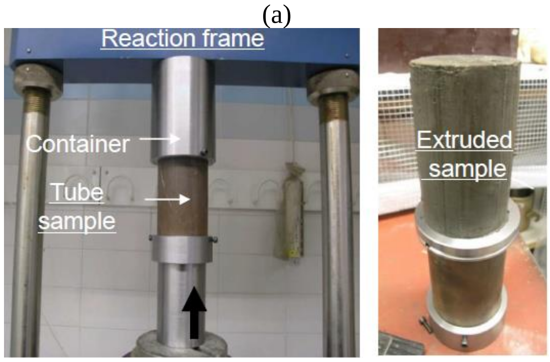

(b)

Figure 4. Sample preparation. (a) insertion of 1mm thin oedometer ring. (b) extrusion of soil sample for triaxial testing

Table 3. Initial conditions and normalized void ratio measured from CRS and CK_0U tests

Borehole & sampler type	Depth (m)	Test	e_0	$\Delta e/e_0$
BH1 Shelby (88mm)	5.5**	CRS 1	0.82	0.183
		CRS 2	0.85	0.231
		CRS 3	0.79	0.195
	14	TXR 1	0.55	0.085
		CRS 1	0.52	0.035
		CRS 2	0.47	0.039
BH2 Shelby (80mm)	14	TXR 1	1.10	0.134
		TXR 2	1.00	0.132
		CRS 1	1.11	0.067
		CRS 2	1.13	0.052
		CRS 3	1.18	0.049
BH3 Fixed-piston (100mm)	14	TXR 1	1.19	0.120
		CRS 1	1.21	0.083
		CRS 2	1.27	0.051
		CRS 3	1.24	0.060
BH4 Fixed-piston (80mm)	5.5	CRS 1	0.71	0.057
		CRS 2	0.71	0.050
		CRS 3	0.69	0.057
	14	TXR 1	0.92	0.086
		TXR 2	1.15	0.125
		CRS 1	1.14	0.084
		CRS 2	1.29	0.071
		CRS 3	1.32	0.062

***tube cut along its longitudinal axis with a hand grinder*

4. Analysis of the CT scans

Figures 5 and 6 present representative profiles of mean CT value, standard deviation and *CoV* for tube specimens summarized in Table 3. These figures include profiles for three different RoIs defined by inner diameters of 40 mm (similar to the diameter of triaxial specimens), 50 mm (similar to the diameter of CRS samples) and 60 mm. The RoI given by d=60mm is included here to consider the fact that, in some cases, triaxial samples were trimmed from locations within the slice different from its center. This aspect is discussed below. Location of CRS and triaxial samples are also included. Figure 5 shows the profiles for the 88mm Shelby sample (BH1) obtained from z =5.5m. The mean CT value ranges between 1100-1400 HU with higher values observed at top and bottom ends. The standard deviation shows an average value around 100 HU with peak values of 250 HU located at 480 mm from the base. The *CoV* ranges between 0.08 - 0.14 at the central part of the tube. Peaks in *CoV* are consistent with the large standard deviation observed at the same locations.

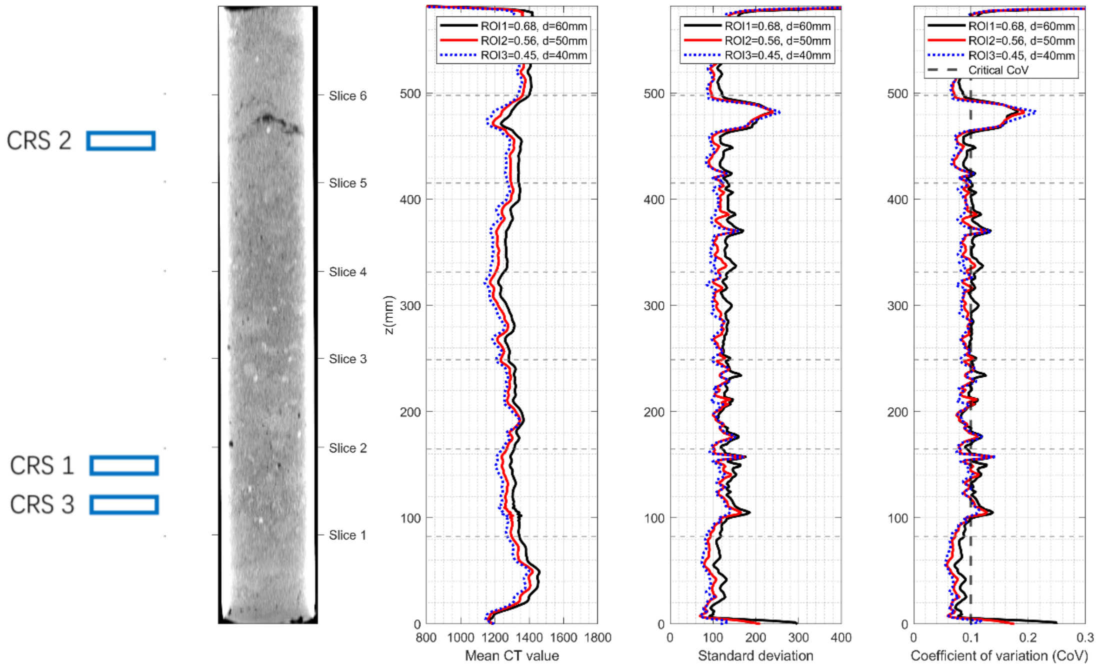

Figure 5. CT profiles for 88mm Shelby tube (BH1) retrieved from z = 5.5m.

Figure 6 shows the profiles for the 100mm fixed-piston sample (BH3) obtained from z=14.5m. The mean CT values varies around 1100 HU with higher values observed at top and bottom ends. The presence of a cobble (white inclusion located at z ≈ 430mm) causes a peak in the mean CT, standard deviation and *CoV* profiles. The standard deviation ranges around 100 HU with a peak value of 300 HU observed at the location of the cobble. The *CoV* varies around 0.09 – 0.12 for the central part of the specimen.

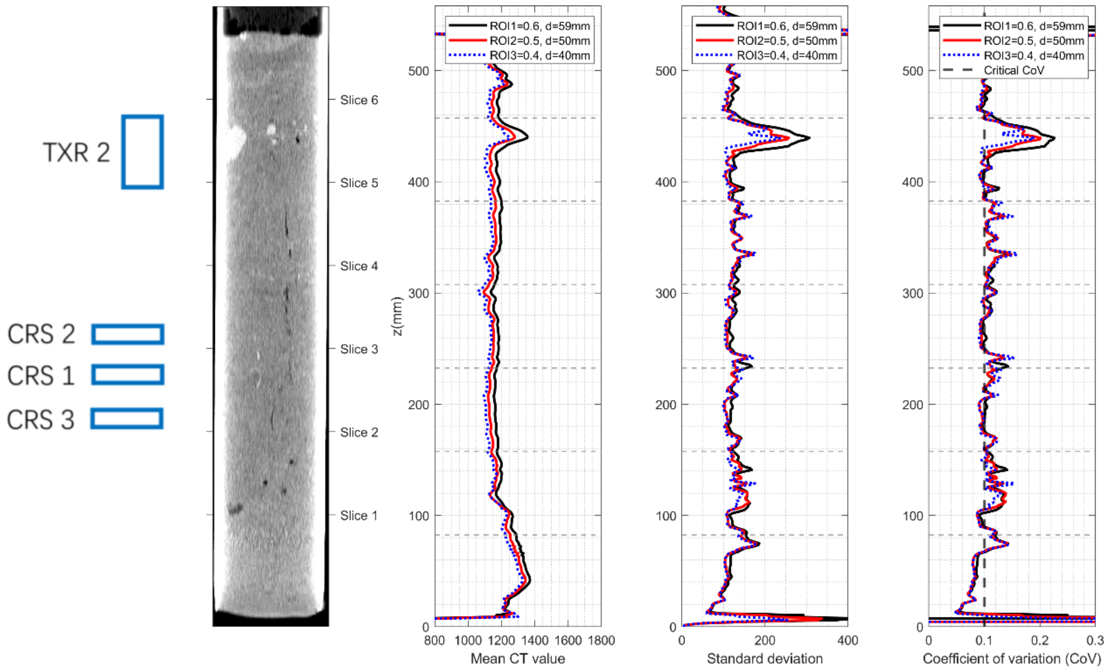

Figure 6. CT profiles for 100mm fixed-piston sample (BH3) retrieved from z=14.5m.

5. Sample quality assessment

The profiles described in the previous section give some hints on the homogeneity of tube specimens and provide preliminary insights for the selection of soil samples for laboratory testing. Nevertheless, a link should be established between the statistical parameters obtained from the analysis of CT scans with existing sample quality indicators. Ouyang et al. (2024) demonstrate that, for the high plasticity Ballina clay from Australia, there is a positive correlation between the *CoV* and the sample quality indicator $\Delta e/e_0$ proposed by Lunne et al. (1997). Ouyang et al. found that values of *CoV* lower than 0.1 represent soil specimens rated as *very good to excellent* and *good to fair*.

Following the same approach, estimates of *CoV* for CRS and triaxial specimens are compared here with values of $\Delta e/e_0$ reported in Table 3. The definition of the *CoV* for this comparison must consider volume of soil used in the mechanical test which implies a ratio between the volume of the tested specimen and the volume of soil selected in the estimation of the *CoV*, equal to $V_{sample\ tested} / V_{CoV} = 1$ (Ouyang et al., 2024).

The same approach was followed in this study with all CRS specimens. On the other hand, the natural heterogeneity of the silty deposits caused problems for the selection of the best location within the 120mm long segments from which 38x76mm triaxial samples were trimmed. In most cases, the centerline of the triaxial sample did not coincide with the centerline of the tube sample due to the detection of fissures, shells or defects during the trimming process. To cover for this the region analysed from the CT to compute the *CoV* was larger than the triaxial specimens. With a RoI defined by a diameter of 60 mm leading to a ratio $V_{sample\ tested} / V_{CoV} = 0.42$.

It is important to note that the *CoV* estimated for CRS and triaxial specimens is the average *CoV* for the set of 2D slices that compose the tested specimens. Hence, this represents a 2D estimation of the *CoV* as discussed in Ouyang et al. (2024). Figure 7 compares the sample quality index $\Delta e/e_0$ and the *CoV* estimated for CRS and triaxial specimens. Results obtained for Ballina clay specimens, represented with empty symbols, are included in this figure for comparison. CRS and triaxial specimens are represented by black squares and red circles, respectively. Overall, the *CoV* increases with $\Delta e/e_0$ following the trend previously established in Ouyang et al. (2024) for Ballina clay. Most CRS specimens display values of *CoV* lower than 0.1 whereas several triaxial samples plot above that limiting value. The positive correlation between *CoV* and $\Delta e/e_0$ observed in Figure 7 for the silty deposits from Castello d'Empuries indicate that, in the absence of additional data, the separation between good quality samples from disturbed specimens (that should be discarded for mechanical testing) may be defined by *CoV*=0.1. This threshold value encompasses zones 1 and 2 defined by Lunne's et al., i.e. $\Delta e/e_0 < 0.07$ for soils with OCR<2.

The three black squares enclosed by a dashed ellipse in Figure 7 represents CRS specimens from the 88mm Shelby tube (BH1) retrieved from z=5.5m. Although the *CoV* is slightly higher than 0.1, the image variability seems small considering the large $\Delta e/e_0$ measured in the oedometer tests. This sample was the first tube tested after the sampling campaign and the soil was extruded by cutting the tube along its longitudinal direction as explained in Section 3.3. Pictures of the tube after cutting are shown in Figure 8. The very soft (muddy) sample was disturbed during the process of soil extrusion, perhaps due to suction effects generated when the upper half of the tube was removed. Of course, the likely damage caused by this extrusion procedure could not be reflected on the tomographic images of the tube.

The experience gained after the extrusion of this tube sample motivated the modification of the extrusion protocol which was replaced by slicing the tube into small segments as described in Section 3.3. Slicing prior soil extrusion has been found as a cost-effective method not only in low plasticity silty soils like those tested here but also in high plasticity marine soft clays (see Pineda et al., 2014).

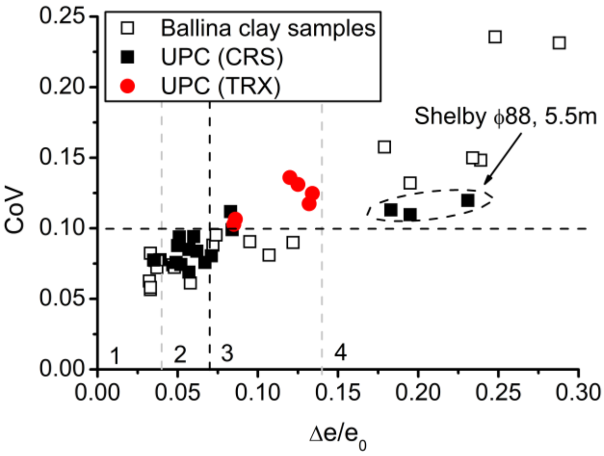

Figure 7. Correlation of CoV and $\Delta e/e_0$

Figure 8. Cutting and sample trimming for the 88mm Shelby tube (BH1) retrieved from z = 5.5m.

6. Concluding remarks

The paper discussed the performance of a novel quantitative method developed to evaluate sample quality in soft soils. This new technique was applied to low-plasticity Mediterranean deltaic deposits found in the region of Castello d'Empuries at the Costa Brava, in Catalonia (Spain). CT scans of Shelby tubes and fixed-piston samplers were used to estimate statistical parameters which, in turn, allowed the assessment of the sample quality. Comparison against estimates of the sample quality index $\Delta e/e_0$ showed good agreement, indicating the good performance of the proposed method not only to high plasticity soft clays but also to low plasticity clayey silt deposits.

7. References

Arroyo, M., Pineda, J.A., Sau, N., Devincenzi, M. & Perez, N. (2015) Sample quality exaination on silty soils. In Proc. XVI European Conference on Soil Mechanics and Geotechnical Engineering, Edinburg, UK, 2873-2878.

Baligh, M. M., Azzouz, A. S. & Chin, C. T. (1987). Disturbance due to 'ideal' tube sampling. J. Geot. Engn 113, No. 7, 739–757.

Clayton, C. R. I., Siddique, A. & Hopper, R. J. (1998). Effects of sampler design on tube sampler disturbance-numerical and analytical investigations. Géotechnique 48, No. 6, 847–867.

Díaz, J. I. & Ercilla, G. (1993). Holocene depositional history ofthe Fluviá—Muga prodelta, northwestern Mediterranean Sea. Marine Geology, 111(1),83-92.

Duliu, O.G. (1999) Computer axial tomography in geosciences: an overview. Earth Science Reviews, 48, 265-281.

Hvorslev, M. J. (1948) Subsurface exploration and sampling of soil for civil engineering purposes. Vicksburg, MS, USA: Waterways Experiment Station, U.S. Army Corps of Engineers

Ladd, C. & DeGroot, D. (2003) Recommended practice for soft ground site characterization: Arthur Casagrande Lecture. In Proc. 12th PanAmerican Conference on Soil Mechanics and Geotechnical Engineering (eds P.J. Culligan, H.H. Einstein and A.J. Whittle), vol 1, 3-57.

Lim, G.T., Pineda, J.A., Boukpeti, N., Carraro, J.A.H. & Fourie, A. (2019) Effects of sampling disturbance in geotechnical design. Canadian Geotechnical Journal, 56(2), 275-289.

Lim, G.T., Pineda, J.A., Boukpeti, N., Fourie, A. & Carraro, J.A.H. (2018) Experimental assessment of sampling disturbance in calcareous silt. Geotechnique Letters, 8(3), 240-247.

Lunne, T., Berre, T., & Strandvik, S. (1997). *Sample disturbance effects in soft low plastic Norwegian clay*. Symposium on Recent Developments in Soil and Pavement Mechanics.

Monforte, L., Arroyo, M., Carbonell, J. M., & Gens, A. (2022). Large-strain analysis of undrained smooth tube sampling. Géotechnique, 72(1), 61-77.

Osterberg, J.O. (1973) An improved hydraulic piston sampler. Proc. 8th Int. Conf. Soil Mech. And Foundation Eng., Moscow, Volume 1.2, 317-321.

Ouyang, K., Pineda, J.A., Kelly, R.B., Bates, L. & Wilson, L. (2024) Quantitative sample quality assessment in soft soils via CT scanning. Geotechnique (submitted)

Pineda, J.A., Arroyo, M., Sau, N., Perez, N. & Gens, A. (2012a) Testing block samples from silty deposits. In Proc. Int. Conference on Geotechnical and Geophysical Site Characterization, ISC4, Coutinho and Mayne (eds), 1815-1823.

Pineda, J.A., Sau, N. & Arroyo, M. (2012b) Ensayos de laboratorio sobre materiales de la zona de Castello de Empuries. Internal Report, UPC, Barcelona.

Pineda, J.A., Suwal, L. & Kelly, R.B. (2014) Sampling and laboratory testing of Ballina clay. Australian Geomechanics Journal, Vol 49(4), 27-40.

Pineda, J.A., Liu, X-F. & Sloan, S.W. (2016a) Effects of tube sampling in soft clay: a microstructural insight. Geotechnique, 66(12), 969-983.

Pineda, J. A., Suwal, L. P., Kelly, R. B., Bates, L., & Sloan, S. W. (2016b). Characterisation of Ballina clay. *Géotechnique, 66*(7), 556–577. https://doi.org/10.1680/jgeot.15.P.181

Sau, N. (2013) CAT scanner as a tool for geotechnical sample inspection. Master thesis in Geotechnical Engineering. Universitat Politecnica de Catalunya, BarcelonaTech, UPC, Spain.